uc3m | Universidad Carlos III de Madrid

e-Archivo

This is a postprint version of the following published document:

Yunta, J., Garcia-Pozuelo, D., Diaz, V., & Olatunbosun, O. (2019). Influence of camber angle on tire tread behavior by an on-board strain-based system for intelligent tires. *In Measurement, 145*, 631–639

DOI: 10.1016/j.measurement.2019.05.105

© 2019 Elsevier Ltd. All rights reserved.

This work is licensed under a Creative Commons Attribution-NonCommercial-NoDerivatives 4.0 International License.

Influence of camber angle on tire tread behavior by an on-board strain-based system for intelligent tires

J. Yunta[a]*, D. Garcia-Pozuelo[b], V. Diaz[b] and O. Olatunbosun[c]

[a]*Phd. In Mechanical Engineering and Industrial Management;*
[b]*Department of Mechanical Engineering, Research Institute of Vehicle Safety (ISVA), Universidad Carlos III de Madrid, Avd. De la Universidad, Madrid, 28911, Spain;*
[c]*School of Mechanical Engineering, University of Birmingham, Edgbaston B15 2TT, UK.*

ARTICLE INFO

Article history:
Received 00 December 00
Received in revised form 00 January 00
Accepted 00 February 00

Keywords:
Intelligent tires
Strain gauges
Tire deformation
Camber angle

ABSTRACT

Tires are a key sub-system of vehicles that have a big responsibility in comfort, fuel consumption and traffic safety. Nevertheless, current tires are just passive rubber elements which do not contribute actively to improve the driving experience or the vehicle safety. The lack of information that tires provide during driving is the main reason to develop an intelligent tire, which could provide useful information to other systems and become an active safety system. In this paper, an experimental tire strain-based system is used to measure tire tread deformation by means of strain gauges. Tests under different working conditions such as vertical load or slip angle considering a certain camber angle have been carried out using an indoor tire test rig. The results prove that the camber angle has a significant effect on strain signal, so it should be considered for tire working conditions estimation purposes.

© 2018 xxxxxxxx. Hosting by Elsevier B.V. All rights reserved.

1. Introduction

Pneumatic tires are the only components transferring the load from the vehicle to the road, therefore, their performance has great influences on the vehicle dynamics, the driving experience or the active safety systems. In addition, many parameters have influence on the tire performance, such as the vertical load, the rolling speed, the temperature, the slip angle or the camber angle. The wealth of information about tire working conditions potentially available from the tire could be used by current control systems in order to improve their effectiveness to avoid potentially hazardous situations where drivers partially lose control of the vehicle. The possibility of using tires as a source of information is usually encompassed by the term intelligent tires. An intelligent tire would have the final objective of monitoring in real-time the longitudinal and lateral forces at the contact patch, the potential adherence, the slip angle, etc. In this field, the Apollo Consortium [1] summarized some years ago the potential benefits thereof, showing that the intelligent tire could be a key element in future vehicles (see Figure 1). The TPMS (Tire Pressure Monitoring System) has been the only advance in mass production [2], but the prospects of the intelligent tire go well beyond that of TPMS with the increasing demand of the automotive industry and the society for safer vehicles.

In recent years, there has been an increasing amount of literature on the possibility of getting information from tire deformation or other parameters by using different technologies. For instance, Surface Acoustic Wave (SAW) sensors [3-5], optical sensors [6-9], piezoelectric sensors [10,11], accelerometers [12-15] or capacitive sensors [16-20]. Although they demonstrated the capability to provide information about tire working conditions from tire behaviour, they usually have some limitations such as energy consumption, robustness or dependency of the tire-rim relative position. There is a large volume of published studies indicating that strain sensors meet the requirements to achieve an advanced intelligent tire system from strain measurement [21-27]. In addition, strain sensors are less expensive and bulky than other sensors to measure the tire's deformation, which is associated with most of the tire working conditions.

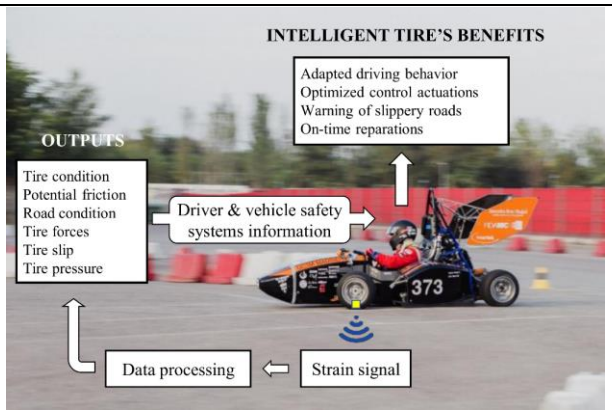

Figure 1. Potential benefits of intelligent tires (UC3M FSAE race car).

The price of strain gauges as well as the robustness thereof have demonstrated that they are suitable for developing the intelligent tire. In addition, since these sensors are basically flexible metallic foil that are very slim, it could be possible to embed them into the tire layers, increasing the robustness of the system and integrating them into the tires' mass production.

Apart from choosing the most suitable sensor technology for the future viability of intelligent tires, more obstacles must be overcome. On the one hand, problems regarding the intrinsic nature of tires, which are a complex composite structure, made up of rubber material and steel wires that behaves in a non-linear way, makes it difficult to find relations between sensor signals and tire working conditions. On the other hand, it is necessary to consider compatibility problems due to the tire working environment, such as the data transmission [10,28], the power requirements

of all the electronic devices [29-31] and the methodology and equipment used in order to implement the above mentioned elements with a minimum level of reliability to ensure that the systems will work during the tire life cycle.

In this paper, a series of experiments by means of an on-board strain sensor system and an indoor tire test rig have been carried out. These devices were selected to measure strain dynamic behavior based on tire working conditions (vertical load, rolling speed, slip angle and camber angle), which define along with the road conditions the tire dynamic behavior. This work is a continuation of the experiments carried out to measure the tire's deformation on the inner surface of the tire tread [22-25], where the relation between tire working conditions and some significant points of strain curves was demonstrated. However, these experiments were carried out without camber angle, so the possibility of estimating the vertical load or the slip angle could depend also on the influence of the camber angle on strain curves peaks. For this reason, this work concentrates on the influence of rolling speed, vertical load and slip angle on strain curves considering a fixed camber angle to elucidate how this parameter and the tire-road contact can affect the sensors' signals.

2. Materials and methods

2.1. Strain-based experiment setup

The equipment used to test the tire was the electro-hydraulic tire test rig shown in Figure 2. This test facility allows to investigate the tire's behavior by changing some working parameters such as the slip angle, the vertical load or the rolling speed in a controlled way. The test rig consists of a drum, two actuators connected to a hydraulic pump for the tire positioning and a mechanical device (see Figure 2b) to change the tire slip angle.

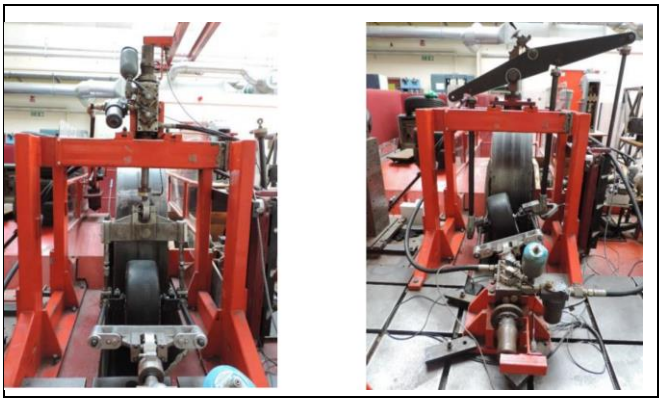

(a) (b)

Figure 2. (a) Indoor tire test rig working in straight line; (b) Device used to apply the slip angle.

The actuators and the speed controller are managed by a specific software (Tiab Limited, Oxfordshire, UK). The rolling speed as well as the test conditions can be downloaded after the test by this software for the data analysis. Finally, it should be highlighted that the drum surface is curved, but due to the large diameter (2.44 m) it has an insignificant effect on the results according to previous studies [32]. The Avon 175/53R13 slick tire, with the sensors attached on the inner part of the tire tread, was used to carry out the tests. The main features are that it is a tubeless tire and soft compound, which allows to install electronic components between the rim and the tire therefore avoiding the risk of damage.

Different from previous work [22-25], this time the tire was placed on the drum's surface with a certain camber angle, which is defined as the angle between the external plane of the wheel and a plane perpendicular to the road. Based on literature survey, the center line of the contact patch due to the camber angle and the pressure distribution is a parabola instead of a straight line due to the lateral displacement [33]. A significant analysis and discussion about the effect of the camber angle on the shape of the contact patch was presented by Cheng et al. [34]. They concluded that it is different (from triangular to trapezoidal) depending on the value of the camber angle and the contact pressure becomes increasingly non-uniform when it increases. Finally, they found that the maximum contact stress of the contact area increases when camber angle also increases. Therefore, it is clear that the camber angle has an important effect on tire performance and tire tread deformation.

As the test rig does not have a specific element to control this parameter, it was done by modifying the position of the vertical actuator up to reach an angle of 5˚ with respect to the tire-road contact point, as shown Figure 3a. This angle was measured using a digital angle meter. When tires are working with a non-zero camber angle, the temperature along the tire tread is not uniform due to one side is supporting more demanding conditions than the other (see Figure 3b). For this reason, despite the fact that this value is quite higher than the ones that are usually used in race cars (in FSAE this angle is usually set between -1º and -3º), it was decided to set a high camber angle to ensure that substantial differences would be found in the results, since this parameter is very aggressive for tire tread wear. Finally, note in Figure 3 that Face B supports higher vertical loads than Face A, which is an important detail for the data analysis.

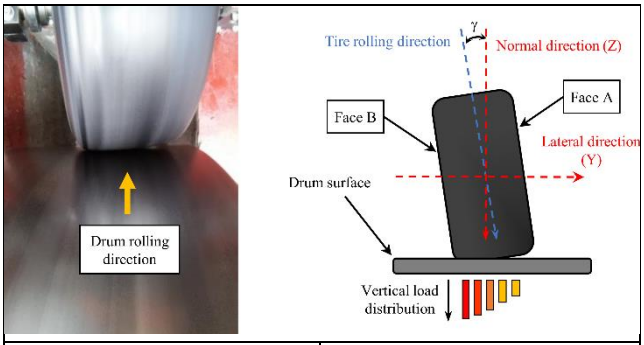

(a) (b)

Figure 3. (a) Top view of the tire rolling with camber angle; (b) The effect of camber angle on vertical load distribution.

Regarding the sensors, some uniaxial strain gauges (FLA type, 6 mm length, Tokyo Sokki Kenkyujo Co., Ltd.) were installed on the inner part of the tire tread and sidewall after carrying out the surface preparation process recommended by the manufacturer, in the same way as for previous works [22-25]. Many different strain gauges and adhesives were tested, including LF series. The results have been very similar in the morphology of the curves and the quantitative differences in the signals haven't been considered as crucial (less than 10%). For this reason, the strain gauges and adhesives which showed better response were chosen to carry out the tests. They were installed in lateral and longitudinal measuring directions at different lateral distances from the middle plane of the tire tread, as shown Figure 4. It should be pointed out that the strain gauges were temperature self-compensated and the temperature changes on the tire are not taken into account in this work because the test conditions have been kept constant in terms of temperature and humidity (23 ◦C and 50% HR), following the recommendations of the strain gauge manufacturer.

Due to the characteristics of the data acquisition system (DAQ), it was necessary to place a resistor between the strain sensors and it to complete the Wheatstone bridge, since part of it was included in the DAQ. For this reason, more strain gauges were installed to have some extra measurement channels, since the centrifugal force could damage the solder joints of the

electrical connections. This fact was corroborated during and after the tests, since it was found that some solder joints were broken during the experiments, so some channels did not measure good data from a certain moment. Thus, only the data obtained by channels numbered in Figure 4, which gave us relevant data during all the test conditions, have been analyzed in depth. There are two channels that did not appear on Figure 4, one to the left of channel 5 in lateral direction (symmetric to channel 2 from the longitudinal middle plane) and another two in longitudinal direction (symmetric to channels 3 and 4 from longitudinal middle plane). The solder joints of those sensors were damage in the middle of the tests set and started measuring inconsistent data. For this reason, they were not considered for the analysis. The robustness of the sensors' wires connection will be an aspect to be improved for future tests.

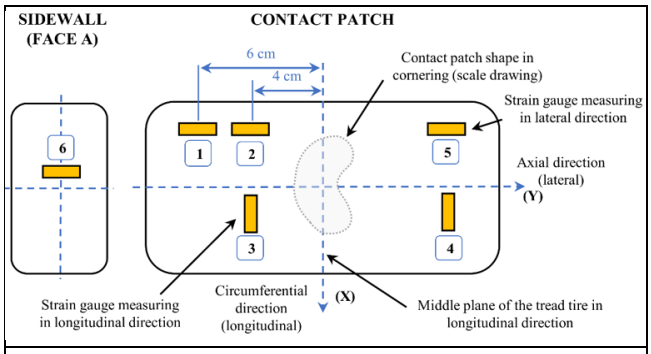

Figure 4. Schematic to indicate the channels' numbers, placement and direction of measurement of strain gauges.

As it is observed in Figure 4, the influence of the distance to the middle plane can be studied by the comparison between the data provided by channels 1 and 2 in lateral measuring direction and channels 3 and 4 in longitudinal measuring direction. Note that, channels 1, 2 and 3 are placed in the side that is unloaded during the tests (see Figure 3), while channels 5 and 4 are placed on the overloaded side due to the camber angle. In the same way, the influence of camber angle can be analyzed by means of the comparison between channels 1 and 5, which are placed at the same distance from the middle plane. Figure 4 also shows the typical shape of the contact patch when a tire is rolling in cornering conditions. Although this shape changes with the camber angle, it could explain the behavior of channels depending on the side in which they are placed. In cornering tests, it is assumed that channels 1, 2 and 3 are placed on the outer part of the contact patch while channels 4 and 5 are on the inner part.

Finally, it should be taken into account that channel 6 was attached to the sidewall that is unloaded, measuring in longitudinal direction considering the axis shown in Figure 3b. The objective was to elucidate if a strain sensor placed on this part could provide more useful information than the ones that are installed on the tire tread, since previous studies [10] concluded that data measured on the outer part of the sidewall are related with the slip angle.

Figure 5a illustrates the installation of the uniaxial strain sensors. It was made using the M-Bond AE 10 adhesive, which is recommended for this kind of application, so it can be assumed that the stiffness of the strain gauges does not cause local stiffening effects. The strain gauge's length is 6 mm with a resistance of 120 Ω and the resolution 0.001 με. Some tire patches and multipurpose adhesive tape were used to fasten the cables to the tire, avoiding the strain sensors to be damaged, as shown Figure 5b.

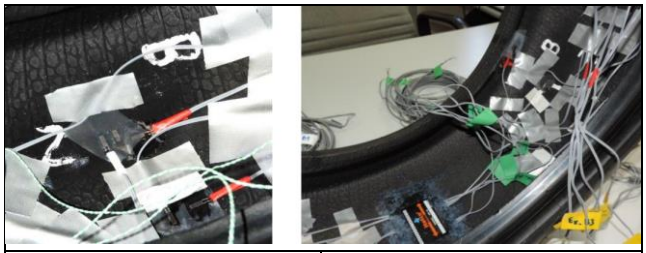

(a) (b)

Figure 5. (a) Strain gauges attached on the inner of the tire tread; (b) Wires grabbed with tire patches and labelled.

Regarding the DAQ, the Slice Micro DTS® (Diversified Technical Systems, CA, USA). was used to carry out the tests. It consists of three modules: the base, that comprises the microprocessor, the amplifier and the A/D converter; signal conditioning and two more slices that allow to connect a maximum of three channels each, as shown Figure 6.

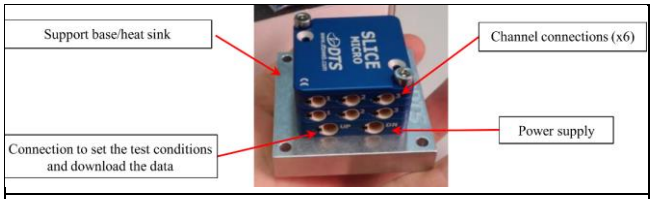

Figure 6. Hardware of the data acquisition system.

The weight (approximately 80 g) and the dimensions (42x42x30 mm) of the device are suitable for this application, since it is possible to take advantage of the space between the rim and the tire installing the DAQ in that space, and its low weight does not imply a great tire unbalance. In addition, this device is designed to carry out experiments in portable conditions, so an external battery can be connected for the energy supply. The Slice Micro DTS® can provide a sampling frequency up to 500 kHz and storage 16 GB of data. For this application, the sampling frequency was set to be 1000 Hz and the working range used covered from -12000 to 12000 με, which are suitable for the tire characteristics and test speeds.

Before starting a test, the DAQ is connected to a computer using the Sliceware DTS® software to set the test conditions and run it at the same time as the software to manage the drum, ensuring the concordance between the data acquired from both parts.

For the attachment of the DAQ and the battery, the EvoCorse X3MAZero rim (unibody) was machined, and a support base as well as a metallic frame for the Slice Micro DTS® was designed and manufactured in aluminum, as shown Figure 7a.

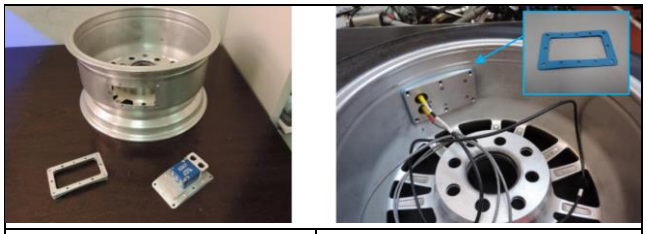

(a) (b)

Figure 7. (a) Machined tire rim and the aluminum base for the DAQ; (b) Connectors to PC and battery.

The function of the frame, which was screwed to the rim, was to allow the support base to be screwed considering the different forces due to the dynamic conditions. The support base was designed considering several aspects. First of all, it should be light but robust, ensuring that the bolts can

support the demanding conditions of the experiments. Secondly, it should have two big holes to allow the cables "up" (to upload data from the DAQ to the computer) and "down" (to configure the DAQ for the test conditions from the computer) to be connected from the outside (see Figures 6 and 7b). Fo this purpose, two connectors were prepared for the requirements of the DAQ. Finally, it should ensure that the DAQ was fixed to the support during the test and the air didn´t leak through the holes or the contact surface between the support and the rim. To do this, a flat seal with a specific design was made using a 3D printer and a rubber filament (see Figure 7b). The possible void between some metallic parts was filled using a liquid material based on silicone. The seal reliability was checked by leaving the tire for three days. After that, the inflation pressure decreased just by 0.1 bar.

Figure 8a shows the Slice Micro DTS® connected to the strain sensors and to the up and down connectors, which pass the connections through the aluminum support. The design of this element makes it possible to extract the device easily and check the connections from time to time during the tests.

(a) (b)

Figure 8. (a) Channels connected to the DAQ; (b) Battery attached to the rim.

The energy supply for the DAQ consist of a portable 12V battery with a capacity of 2200 mAh that, due to the low power consumption of the device, allows to carry out test for several hours. After that, the battery can be disconnected from the Slice Micro DTS® and plugged to the charger. As it is shown in Figure 8b, a plastic support was also made using a 3D printer and PLA filament. The density (i.e. weight) and the hardness of this printing material make it suitable for this application. This element was also screwed to the rim by bolts.

2.2. Strain-based experiment setup

The operational range of parameters used for the test are:

- Tire inflation pressure: 1 bar;
- Tire preload: 250 N – 1000 N;
- Tire speed: 10 km/h – 30 km/h;
- Tire camber angle (γ): 5°;
- Tire slip angle (α): 0° – 8°;

Regarding the preload, speed and slip angle, they were performed at 250 N, 10 km/h and 2° intervals, respectively. These intervals provide results for 48 different test conditions for every channel. It is also noteworthy that some preliminary tests were made to observe if there were differences in the data for different inflation pressure. As a major result, it was found that the influence of inflation pressure on strain data is low in comparison with other parameters such as vertical load, which itself can have some fluctuations due to the little slips that occurs at the contact surface between the tire and the drum. As a consequence, in the same way as in previous studies [22-24], the possible differences on strain peaks due to the inflation pressure are masked, since the vertical load is much more influential on strain data than inflation pressure. For this reason, the inflation pressure was set to be 1 bar for all the tests.

It should be also pointed out that, although the rolling speed could be considered low, it has to be taken into account that the race cars that use this kind of tires (see Figure 1) take part in the FSAE championship, where the average speed is frequently under 50 km/h. Thus, most of the conditions in which the tire can be involved along the circuit have been covered.

Finally, before carrying out the tests, the tire was warmed up by leaving it rolling for several minutes, checking that the laboratory temperature was similar in order to keep the conditions as constant as possible. In total, the tire was tested for over 30 hours, since it was left rolling for each set of conditions for adequate time for getting repeated data samples.

3. Materials and methods

The experimental data analysis allows to study the effect of tire working conditions on tire tread behaviour and make comparisons between the tire rotational cycles to visualize these effects. The variation in strain data collected can provide information to identify the variation of the tire working conditions considering the effect of camber angle on strain channels taking into account the distance to the longitudinal middle plane of the tire.

Figure 9 shows three rotational cycles of the tire for channels measuring in longitudinal and lateral directions. For the longitudinal ones, it is observed that a maximum tensile peak (A) is obtained when the sensors are passing through the tire contact patch. Conversely, lateral channels normally show a maximum compressive peak (C). The interval between peaks A and B correspond to the time that the tire takes to complete a full revolution, so it is directly related to the rolling speed. On the other hand, when the sensors are getting closer to the contact patch, they show maximum tensile or compressive peaks depending on the measuring direction. In the case of longitudinal channels, they show two compressive peaks at the beginning (D) and ending (E) of the contact patch. Lateral channels show two tensile peaks (F and G) when the sensor is getting closer to the contact patch or moving away.

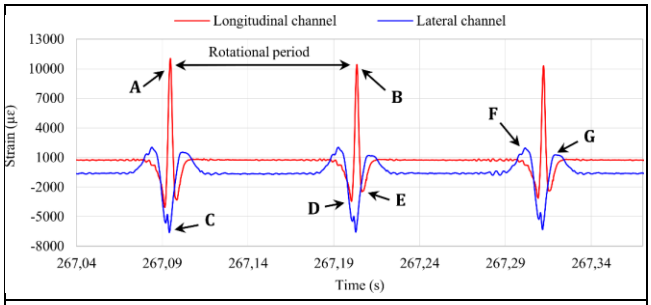

Figure 9. Example of strain curves collected in longitudinal and lateral measuring direction.

As it was previously demonstrated [22-23], although the tire is a complex non-linear system, it is possible to estimate some tire working conditions such as the vertical load or slip angle from these significant points. As it was mentioned, the camber angle influences the way in which the vertical load (that affects, considerably, the strain curve peaks) is distributed through the tread tire. As a consequence, the strain peaks could change due to this effect, so the influence of the camber angle must be considered to keep the possibilities of estimating parameters by estimation methodologies.

Finally, since strain curves are not exactly the same for each testing condition, before starting the data analysis, the representative data curves were obtained taking into account the average strain for each point of the tire rotation cycle, plotting them as a function of the tire rotation angle (360˚) to examine the results (raw data without filtering) from the different channels under identical driving conditions. In the following sections, the most interesting results in straight line and cornering conditions are shown and corroborated with additional experimental tests.

3.1. Straight line rolling conditions

In this section, the most significant results in straight line conditions (slip angle equal to 0˚) focusing on the influence of camber angle on strain data are shown. To illustrate this, a comparison has been carried out between the different channels and test conditions. Figure 10 shows the strain curves of lateral channels 1 and 2, which are placed at 6 and 4 cm from the longitudinal middle plane. The schematic showed in Figure 4 has been included in the following figures for better understanding.

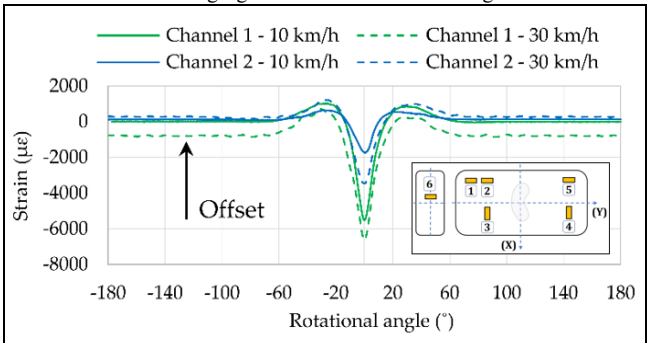

Figure 10. Comparison of curves at different speeds in channels 1 and 2 (250 N, γ = 5º and α = 0º).

As it is observed, channel 1, which is placed farther away from the longitudinal middle plane than channel 2, shows a higher compressive strain peak (almost double) in the middle of the contact patch (rotational angle = 0˚), even taking into account that channel 2 is closer to the middle plane, and therefore, to the overloaded side of the contact patch. Moreover, it seems that speed influences channel 2 to a greater extent than channel 1 either the beginning and ending of the contact patch or the maximum compressive peak. However, having a look to the offset values, those that are measured by the sensors away from the contact patch, it is clear that speeds affect channel 1 more than channel 2, not only regarding the differences between both channels, but also concerning the differences between strain data at 10 and 30 km/h for each channel probably due to the centrifugal force.

In Figure 11, the comparison between channels 3 and 4, which are placed on different sides of the contact patch (see Figure 4), is shown. In this case, channel 4 shows higher deformation (either for 250 or 500 N) in the maximum tensile peak than channel 3. This fact is probably due to two factors; firstly, channel 4 is placed on the overloaded side of the tire tread due to the camber angle, so it is logical that higher strain values are obtained by this channel; secondly, channel 4 is placed closer to the sidewall, which is a more flexible region considering the typical internal structure of tires. Thus, in the same way as channel 1, to place sensors closer to the longitudinal plane provide higher and more different strain peaks values.

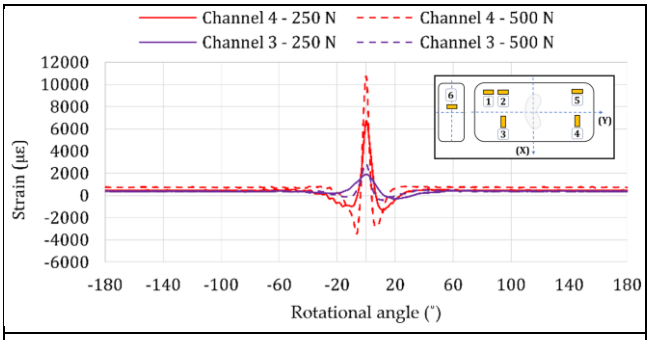

Figure 11. Comparison at different vertical loads in channels 3 and 4 (30 km/h, γ = 5º and α = 0º).

In addition, it is also observed that when vertical load is increased, channel 3 shows smaller differences in the maximum tensile peak than channel 4, so once again, the area of the tire tread that is closer to the sidewall shows higher deformation sensitivity around on this strain peak in terms of vertical load variations. Finally, it should be pointed out that channel 4 also reaches higher values at the maximum compressive points at the beginning and ending of the contact patch.

3.2. Cornering conditions

When cornering, car tires deform laterally and longitudinally, causing changes in the tire tread deformation. As a consequence, the contact patch also deforms in order to drive the vehicle along a certain path, causing a shape similar to the one that is shown in Figure 4. In this way, some of the sensors are passing on the outer part (channels 1, 2 and 3) while the others do it on the inner part of the contact patch (channels 4 and 5). As it will be shown in the following figures, this fact has a great relevance for the channels that measured in lateral direction.

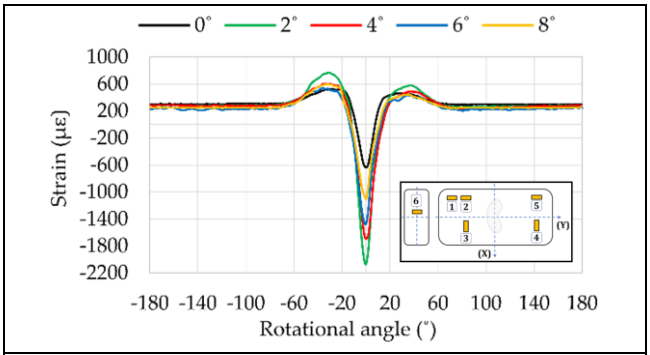

(a)

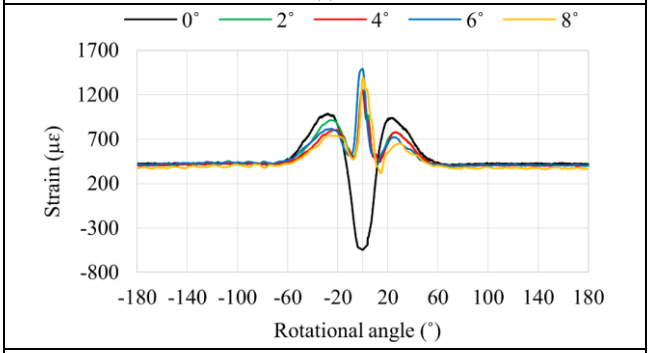

(b)

Figure 12. Comparison at different slip angles in (a) channel 1; and (b) channel 5 (250 N, 10 km/h and γ = 5º).

Figure 12 illustrates a comparison between channels 1 and 5, which are placed at the same cross distance from the longitudinal middle plane (see Figure 4), but channel 1 is placed on the outer part of the contact patch (the zone that is supporting lower vertical load, see Figure 3) while channel 5 is placed on the opposite side.

Channel 5 shows more differences at the beginning and ending of the contact patch than channel 1, but the behaviour of these maximum tensile peaks is quite similar, as shown Figures 12a,b. However, the most interesting results are shown concerning the centre of the contact patch. Normally, lateral channels show a maximum compressive peak when the sensor passes through this area. Nevertheless, in the same way as in previous studies [23, 24], lateral channels placed on the inner part of the contact patch measure maximum tensile peaks instead of a maximum compressive peak when slip angle is different to 0˚ and the vertical load is lower. Since it only appears in cornering conditions. This peak would make it difficult to extract the maximum strain peaks in real time applications, which was the major reason why the channel placed on this side was not chosen for estimation purposes. Since similar results were obtained using a completely different equipment in the past, it can be concluded that lateral channels placed on the inner part of the contact patch are not as useful as it could be expected.

Regarding the influence of camber angle, despite the fact that channels 1 and 5 are placed on opposite sides, they do not show significant differences for any of the significant peaks, but it should be mentioned that maximum tensile peaks at the beginning and ending of the contact patch are slightly higher in channel 1 (Figure 12a) than in channel 5 (Figure 12b). The influence of this parameter in longitudinal channels is more pronounced. In this case, the influence of the camber angle is huge, especially for the maximum tensile peak, where the value is approximately seven times higher in channel 4 than in channel 3 (see Figures 13a,b).

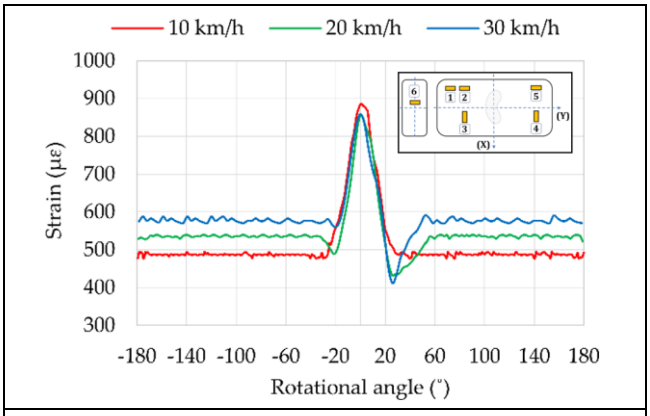

(a)

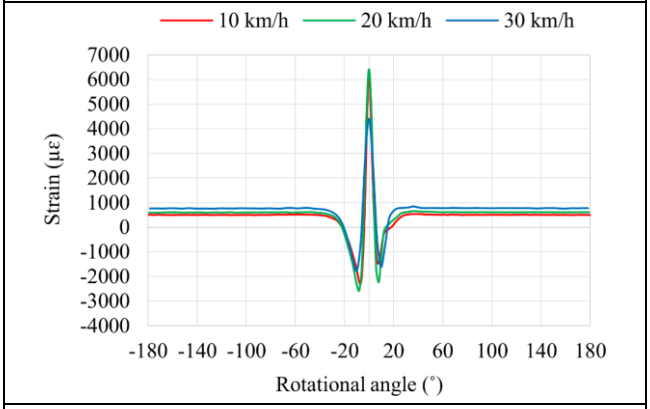

(b)

Figure 13. Comparison at different speeds in (a) channel 3; and (b) channel 4 (250 N, γ = 5º and α = 6˚).

Note that, channels placed in longitudinal direction provide significant and quite clear differences in offset values when rolling speed change, as shown Figure 13a. However, the influence of this parameter on the maximum strain peaks is not linear, neither for the tensile peak nor the compressive ones.

Finally, Figures 14a,b show that the slip angle affects notably, the maximum strain peak at the centre of the contact patch (rotational angle equal to 0˚). Despite the fact that the trend data is not similar in this point, it is observed in Figure 14b that from 4˚ the trend changes, and the maximum tensile peak increases to a lower extent for 6˚ and 8˚. These results could be related with the loss of adhesion, just as it was demonstrated in previous works [22-24].

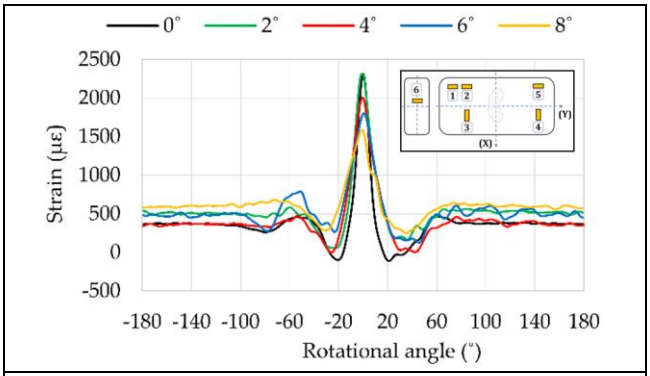

(a)

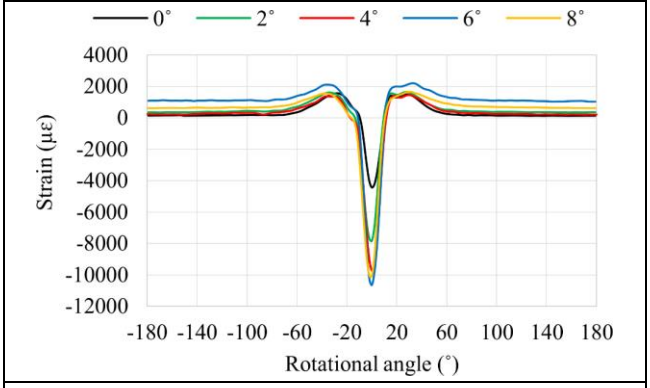

(b)

Figure 14. Comparison at different slip angles in (a) channel 3; and (b) channel 5 (750N, 20 km/h and γ = 5º).

3.3. Sidewall deformation in cornering conditions

Although the majority of studies focus on getting information from the tire tread as it was made herein, some researches have attempted to find relations between the deformation of the tire sidewall and the working conditions. A significant analysis on the subject was presented by Erdogan et al. [10]. In his work, the reliability of sidewall deformation as a source of information to estimate the tire slip angle was demonstrated. To do this, an off-board camera and simple image processing techniques were used. As the future viability of intelligent tire is subjected to the possibility of achieving an on-board implementation of all the equipment, a first approach to obtain information from the sidewall has been carried out. An additional strain sensor was installed on the inner part of the sidewall using the same

equipment as before, as shown in Figure 4. The sensor measured in longitudinal direction considering the axis shown in Figure 3b.

Overall, sidewall strain curves behave in this way (see Figures 15a,b): at the beginning of the contact patch a maximum compressive peak is reached (H); from this peak, the sensor approaches the centre of the contact patch and at which a maximum tensile peak is obtained (I); finally, when the sensor goes further away from the centre of the contact patch, sidewall deformation reduces constantly up to a certain offset value.

Figure 15a shows the influence of rolling speed on sidewall deflection. As it is observed, maximum compressive peak generally decreases as rolling speed increases. However, strain differences at the centre of the contact patch (rotational angle equal to 0˚, point B) are more clear even between 10 and 20 km/h, having the speed the opposite effect on point H than I.

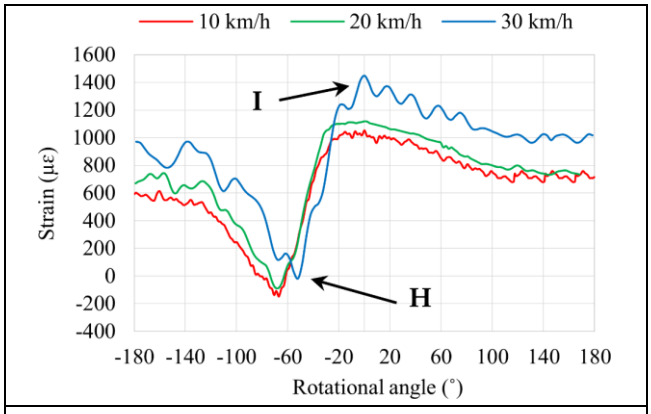

(a)

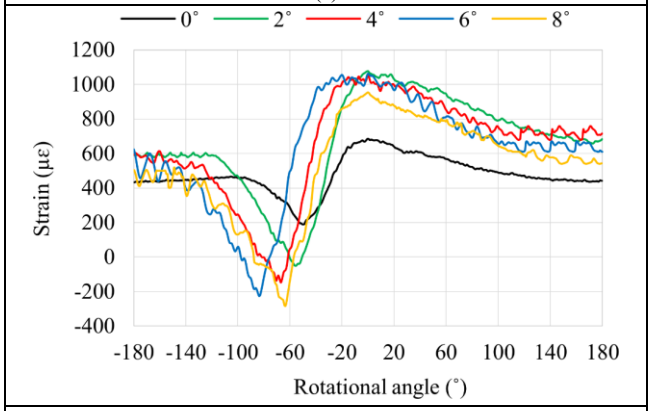

(b)

Figure 15. Comparison at (a) different speeds (250 N, γ = 5º and α = 4º); and (b) different slip angles in channel 6 (250N, 10 km/h, γ = 5º).

Regarding the influence of slip angle, the major differences are shown around the peak H, as shown Figure 15b. When slip angle increases, the maximum compressive peak reaches higher values in a quite linear way. However, strain curves around point I show some fluctuations that makes difficult to extract clear conclusions, although it seems that maximum tensile peaks decrease as slip angle increases.

Despite the fact that information from sidewall deformation could be very interesting for estimation purposes, it should be pointed out that when the tire was tested at higher vertical loads (i.e. the sidewall structure and the sensor were working under more demanding conditions) this channel stopped working. This fact suggests that the strain sensors attached with the abovementioned adhesive in this measuring direction are not suitable for its application on the inner part of the tire sidewall, since the curvature of this area becomes bigger when vertical force increases and the sensor can be damaged.

3.4. Lateral force behavior

In this section, the lateral force behavior collected by a load cell is analyzed. This device was part of the test rig equipment and was placed on the horizontal right arm (see Figure 2b) that hold the wheel. As shown in Figure 16, the lateral force generally increases up to 6º slip angle. The maximum value of lateral force depends directly on the applied vertical force. It is remarkable the parabolic shape of the lateral force curves, which highly resembles the three regions that normally define lateral force curves [35]: linear / elastic (up to 2º), transitional (from 2º to 6º) and frictional (from 6º on). From 6º the tire begins to lose grip and lateral force decreases.

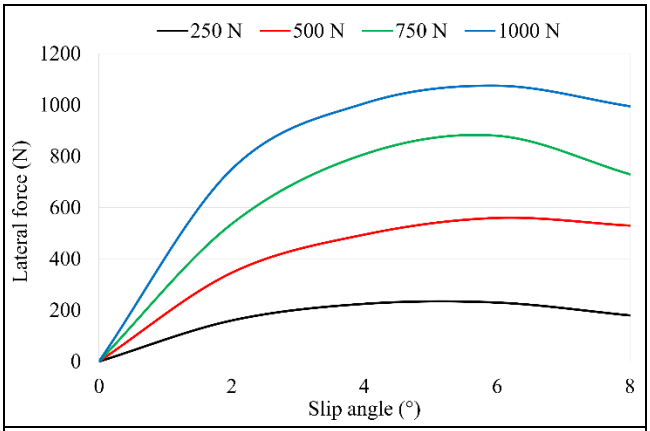

Figure 16. Lateral force behavior (20 km/h and γ = 5º).

The behaviour of lateral force can be expressed as a function of the tire cornering stiffness (K_α), the slip angle (α), the tire camber stiffness (K_γ) and camber angle (γ), as shown Ec. 1 [35,36]:

$F_y = K_\gamma \cdot \gamma + K_\alpha \cdot \alpha$	Ec. 1

According to Figure 16, from 0º to 2º slip angle, both the slip angle and lateral force increase (camber angle remains constant). In the same way, maximum tensile peaks also increase (see Figure 12) because the tire has not reached the limit of adhesion. However, from 2º, the slope of the lateral force curve (for 250 N) is reduced in spite of the slip angle increases in the same proportion. This change in the curve behaviour is be due to the fact that camber angle affects to the lateral force behaviour and tire starts to loss adhesion at the tire contact patch. As the tire's deformation at the contact patch area decreases, the maximum tensile strain collected also decreases (see Figure 12). For these reasons, the results shown in Figure 16 are aligned with the Ec. 1 and the strain data exposed herein.

The behavior of lateral force curves (see Figure 16) is closely linked to the variation of maximum strain data from strain data collected by strain sensors (see Figure 9). In Figure 17a, it is observed that the maximum compressive peak in channel 5 (see Figure 14b) increases up to 6º. From 6º the maximum strain decreases, in the same way that in Figure 16 for lateral force values. During this stage, the tire is beginning to lose grip, and as a consequence, the tire deformation also decreases. Although this behavior is also shown on maximum tensile peaks at the beginning and ending of the contact patch, the changes are less noticeable.

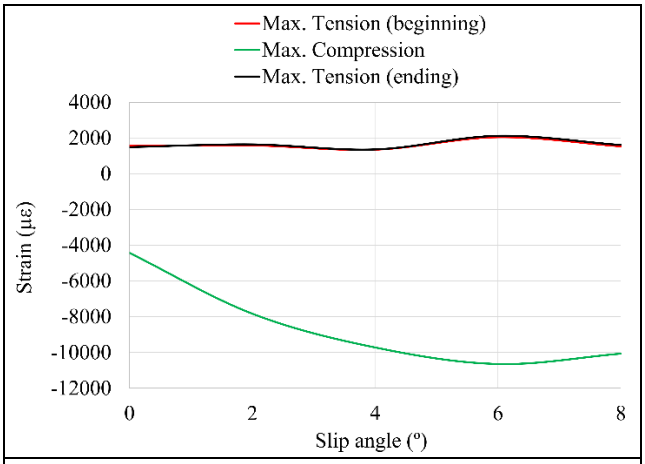

(a)

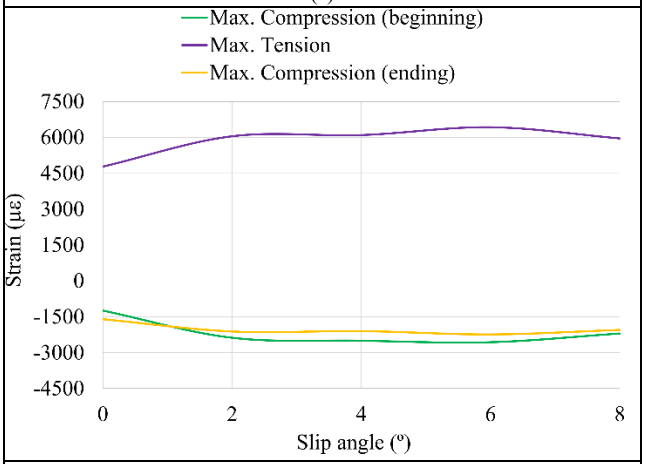

(b)

Figure 17. Maximum strain peaks in (a) channel 5 (750N, 20 km/h and $\gamma = 5º$); and (b) channel 4 (250N, 20 km/h and $\gamma = 5º$).

The similarity in behaviour between lateral force and tire strain curves has a huge potential to develop estimation and control systems, which could provide information to vehicle safety systems. When lateral force starts to decrease (approximately at $\alpha = 6º$), the slope of the curve that represents the maximum compressive peak in channel 5 and 1 change (see Figure 17a,b). In the same way, but in a slighter way, the maximum tensile peaks start to decrease when lateral load also decreases. These relations (in terms of behaviour), that were also found in previous studies [22-24], exist also when a certain camber angle is applied, as it has been demonstrated herein.

4. Discussion

In this paper, an on-board strain based system has been used to measure the tire tread deformation under different working conditions. The tests have been performed on a tire test rig that allows the vertical load, rolling speed and slip angle to be managed. The tire was positioned on the drum considering a constant camber angle for all the tests. In this way, the influence of this parameter on the sensors placed at different distances from the longitudinal middle plane of the tire can be studied.

As the major conclusion, it is clear that the influence of camber angle for estimation purposes must be considered, since it affects the way in which the vertical load is distributed, and then the values of the significant peaks of the strain curves either in longitudinal or lateral measuring direction. Due to the camber angle, the maximum deformation around the centre of the contact patch can be multiplied by several times.

In addition, for the future development of intelligent tires based on strain sensors, some conclusions can be extracted regarding the strain gauge's position and its measuring direction. Channel 1, which is placed closer to the sidewall (i.e. on a more flexible area) on the overloaded side, measured higher strain peaks than channel 2, with the rolling speed having more influence than in channel 2. For this reason, although the area near to the sidewall is more flexible, and therefore, more dangerous for the sensors to be damaged, this area to install the sensors is recommended, being this one of the more interesting conclusion of the study presented in this paper.

In cornering conditions, the influence of the camber angle is more pronounced in the channels placed longitudinally (channels 3 and 4) than laterally (channels 1 and 5). Moreover, as it has been shown, for low vertical loads and cornering conditions, the channel placed on the inner part of the contact patch measured a maximum tensile peak instead of a compressive one. As tires are made essentially of rubber (a viscoelastic material) and multiple layers with different components, it is quite complicated to figure out the way in which the deformation passes through the material from the tire-road contact to the inner surface of the tire tread where the sensors were installed. However, as this behaviour is obtained only in cornering conditions, the self-aligning torque can have some influence on this aspect. Finally, as opposed to straight line conditions, the effect of rolling speed on maximum tensile and compressive peaks is hidden by the influence of other parameters during cornering.

Rolling speed and slip angle show a quite linear relation with strain curves measured on the tire sidewall, but this area seems to deform too much because for the robustness of strain sensors placed in longitudinal direction, so that the sensors placed on this surface became damage during the tests.

As the final aim is to develop an intelligent tire using only one sensor technology, an exhaustive analysis of tire deformation in static conditions is necessary to assess the possibility of estimating tire inflation pressure, because when the tire is rolling, the influence of inflation pressure is not shown due to the vertical load or the rolling speed having more influence on strain data.

Future studies will focus on implementing the effect of camber angle on the estimation system achieved in previous works. Secondly, a detailed study of maximum tensile and compressive strain values for higher speeds and different road surfaces is needed, considering also the effect of accelerating and braking situations that could change the behaviour of strain curves.

References

[1] The Apollo Consortium, Intelligent Tyre for Accident-free Traffic, IST-2001-34372 (2005).
[2] USA, Transportation Recall Enhancement, Accountability and Documentation (TREAD) Act, (2000).
[3] A. Cyllik, T. Strothjohann, G. Scholl, The intelligent tire-applications of the tread sensor, (2001).
[4] J. Eom, H. Lee, B. Choi, A study on the tire deformation sensor for intelligent tires, International Journal of Precision Engineering and Manufacturing. 15 (2014) 155-160.
[5] X. Zhang, F. Wang, Z. Wang, Wei Li, D. He, Intelligent tires based on wireless passive surface acoustic wave sensors, Proceedings. The 7th International IEEE Conference on Intelligent Transportation Systems (IEEE Cat. No. 04TH8749). (2004) 960-964.
[6] A.J. Tuononen , Laser triangulation to measure the carcass deflections of a rolling tire, Measurement Science and Technology. 22 (2011) 125304.
[7] A.J. Tuononen, Optical position detection to measure tyre carcass deflections, Veh. Syst. Dyn. 46 (2008) 471-481.

[8] Y. Xiong, A. Tuononen, The in-plane deformation of a tire carcass: Analysis and measurement, Case Studies in Mechanical Systems and Signal Processing. 2 (2015) 12-18.
[9] A. Tuononen, Y. Xiong, A laser-based sensor system for tire tread deformation measurement, Measurement Science and Technology. 25 (2014) 115103.
[10] G. Erdogan, L. Alexander, R. Rajamani, A novel wireless piezoelectric tire sensor for the estimation of slip angle, Measurement Science and Technology. 21 (2010) 015201.
[11] J. Yi, A Piezo-Sensor-Based "Smart Tire" System for Mobile Robots and Vehicles, IEEE/ASME Transactions on Mechatronics. 13 (2008) 95-103.
[12] G. Anghelache, E.M. Negrus, S. Sorohan, Radial Vibrations of Tire Tread-Band at Different Rolling Speeds, (2000).
[13] G. Anghelache, R. Moisescu, Ş Sorohan, D. Bureţea, Measuring system for investigation of tri-axial stress distribution across the tyre–road contact patch, Measurement. 44 (2011) 559-568.
[14] E. Negrus, Anghelache, G., S. Sorohan, Tire Radial Vibrations at High Speed of Rolling, (1998).
[15] F. Braghin, M. Brusarosco, F. Cheli, A. Cigada, S. Manzoni, F. Mancosu, Measurement of contact forces and patch features by means of accelerometers fixed inside the tire to improve future car active control, Vehicle System Dynamics, 44 (2006) 3-13.
[16] M. Sergio, N. Manaresi, M. Tartagni, R. Guerrieri, R. Canegallo, On road tire deformation measurement system using a capacitive-resistive sensor, Proceedings of IEEE Sensors 2003 (IEEE Cat. No. 03CH37498). 2 (2003) 1059-1063 Vol.2.
[17] R. Matsuzaki, A. Todoroki, Passive wireless strain monitoring of actual tire using capacitance–resistance change and multiple spectral features, Sensors and Actuators A: Physical. 126 (2006) 277-286.
[18] R. Matsuzaki, T. Keating, A. Todoroki, N. Hiraoka, Rubber-based strain sensor fabricated using photolithography for intelligent tires, Sensors and Actuators A: Physical. 148 (2008) 1-9.
[19] R. Matsuzaki, N. Hiraoka, A. Todoroki, Y. Mizutani, Analysis of Applied Load Estimation Using Strain for Intelligent Tires, Journal of Solid Mechanics and Materials Engineering. 4 (2010) 1496-1510.
[20] S. Cao, S. Pyatt, J.C. Anthony, I.A. Kubba, E.A. Kubba, O. Olatunbosun, Flexible Bond Wire Capacitive Strain Sensor for Vehicle Tyres, Sensors. 16 (2016).
[21] H. Morinaga, Y. Wakao, Y. Hanatsuka, A. Kobayakawa, The possibility of intelligent tire (Technology of contact area information sensing), (2006).
[22] D. Garcia-Pozuelo, O. Olatunbosun, J. Yunta, X. Yang, V. Diaz, A Novel Strain-Based Method to Estimate Tire Conditions Using Fuzzy Logic for Intelligent Tires, Sensors. 17(2), 350 (2017).
[23] D. Garcia-Pozuelo, J. Yunta, O. Olatunbosun, X. Yang, V. Diaz, A Strain-Based Method to Estimate Slip Angle and Tire Working Conditions for Intelligent Tires Using Fuzzy Logic, Sensors. 17(4), 874 (2017).
[24] J. Yunta, D. Garcia-Pozuelo, V. Díaz, O. Olatunbosun, A Strain-Based Method to Detect Tires' Loss of Grip and Estimate Lateral Friction Coefficient from Experimental Data by Fuzzy Logic for Intelligent Tire Development, Sensors, 18(2), 490 (2018).
[25] X. Yang, O. Olatunbosun, D. Garcia-Pozuelo Ramos, E. Bolarinwa, Experimental Investigation of Tire Dynamic Strain Characteristics for Developing Strain-Based Intelligent Tire System, SAE Int. J. Passeng. Cars - Mech. Syst. 6. 97-108 (2013).
[26] X. Yang, O. Olatunbosun, D. Garcia-Pozuelo, E. Bolarinwa, FE-Based Tire Loading Estimation for Developing Strain-Based Intelligent Tire System, (2015).
[27] S.J. Kim, K. Kim, Y. Yoon, Development of a tire model based on an analysis of tire strain obtained by an intelligent tire system, International Journal of Automotive Technology. 16 (2015) 865-875.
[28] R. Matsuzaki, A. Todoroki, Wireless Monitoring of Automobile Tires for Intelligent Tires, Sensors. 8 (2008).
[29] K.B. Singh, V. Bedekar, S. Taheri, S. Priya, Piezoelectric vibration energy harvesting system with an adaptive frequency tuning mechanism for intelligent tires, Mechatronics. 22 (2012) 970-988.
[30] O. Yilmazoglu, M. Brandt, J. Sigmund, E. Genc, H.L. Hartnagel, Integrated InAs/GaSb 3D magnetic field sensors for "the intelligent tire", Sensors and Actuators A: Physical. 94 (2001) 59-63.
[31] O. J. Jousimaa, Y. Xiong, A. J. Niskanen, A. J. Tuononen, Energy harvesting system for intelligent tyre sensors, 2016 IEEE Intelligent Vehicles Symposium (IV). (2016) 578-583.
[32] C. Wei, O.A. Olatunbosun, Transient dynamic behaviour of finite element tire traversing obstacles with different heights, J. Terramech. 56 (2014) 1-16.
[33] S. Srinivasa Rao, K. Ramji, M.K. Naidu, Analytical approach for the prediction of steady state tyre forces and moments under different normal pressure distributions, Journal of Terramechanics. 49 (2012) 281-289.
[34] G. Cheng, W. Wang, G. Zhao, Y. Guan, Z. Wang, Influence of Camber Angle on Rolling Radial Tire under Braking State, Procedia Engineering. 15 (2011) 4310-4315.
[35] W.F. Milliken, D.L. Milliken, Race Car Vehicle Dynamics; SAE International: Troy, MI, USA, 1995.
[36] T.D. Gillespie, Fundamentals of vehicle dynamics; SAE International; Warrendale, 1992.